I. Troch, F. Breitenecker, eds. ISBN 978-3-901608-35-3

DETERMINATION OF THE DYNAMIC BEHAVIOR OF AN ELASTO-HYDRODYNAMIC BEARING

E. Berghammer[1], O. Grieshofer[1], K. Mayrhofer[2], R. Minichmayr[2]
[1]Linz Center of Mechatronics GmbH, Linz, Austria;
[2]Siemens VAI Metals Technologies GmbH & Co , Linz, Austria

Corresponding Author: E. Berghammer, Linz Center of Mechatronics GmbH, Altenberger Straße 69, 4040 Linz, Austria; erich.berghammer@lcm.at

Abstract. For industrial applications a lot of process know-how and a good understanding of the dynamic behavior of all the individual components and overall mechanical systems are of high importance. Usually, the systems parameters describing the relevant behavior have been determined through extensive technical experiments for using the results in complex simulation models. In many cases a more flexible and efficient method is to set up appropriate mathematical models and to extract the required parameters from them.
In this paper a model for a special hydrodynamic bearing will be presented, which has been developed for industrial applications. Furthermore, the present paper will show some advantages of implementing separate modules for the physical characteristics of a hydrodynamic bearing. Under certain conditions it is possible to calculate the deformation of the mechanical components and the pressure of the lubricant within the bearings gap independently. Following with a procedure for the automatically creation of the Finite Element models according to the given guidelines and the method to reproduce surface deformations by influence matrices. Finally, the paper describes the identification of the dynamic behavior of a hydrodynamic bearing by numerically solving of the equilibrium-state between the pressure distribution and the mechanical deformations.

1 Introduction

Hydrodynamic bearings for industrial applications usually are highly dynamically loaded, like a roll bearing assembly in rolling mills in steel industry. Such applications require high positioning accuracy but are a dominant compliance in mechanical systems. Therefore, a good understanding of the dynamic behavior of such bearings becomes more and more important.

At high pressures in the lubricant and thin film thicknesses, the mechanical bearing components are significantly elastically deformed (shown in Figure 2) what leads to a change of the pressure distribution and the bearing dynamic. This nonlinear coupling is called Elasto-Hydro-Dynamic (EHD).

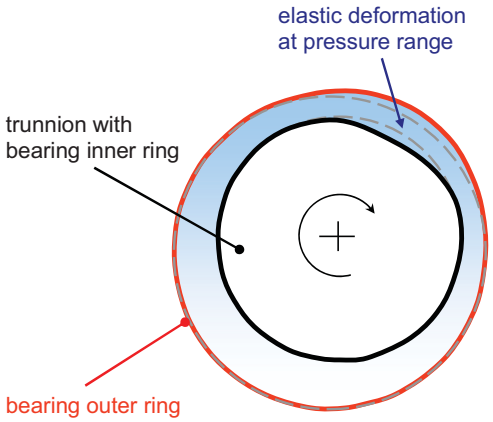

Figure 1. Concept of a deformed hydrodynamic bearing.

This behavior has been investigated carefully and an EHD-bearing model has been set up. The model was used for the numerical determination of the dynamic model parameters at a defined operating point for being able to use the results in complex simulation models.

2 Complete EHD-model of a hydrodynamic bearing

A structure of the developed EHD-bearing model was set up, which allows an independent calculation of the deformations of the mechanical components and the pressure of the lubricant inside the bearing gap. As it is shown in Figure 2, the deformation of the contact surface with oil for both bearing rings is included, as well as the elastic deflection of the shaft, in particular for the trunnion.

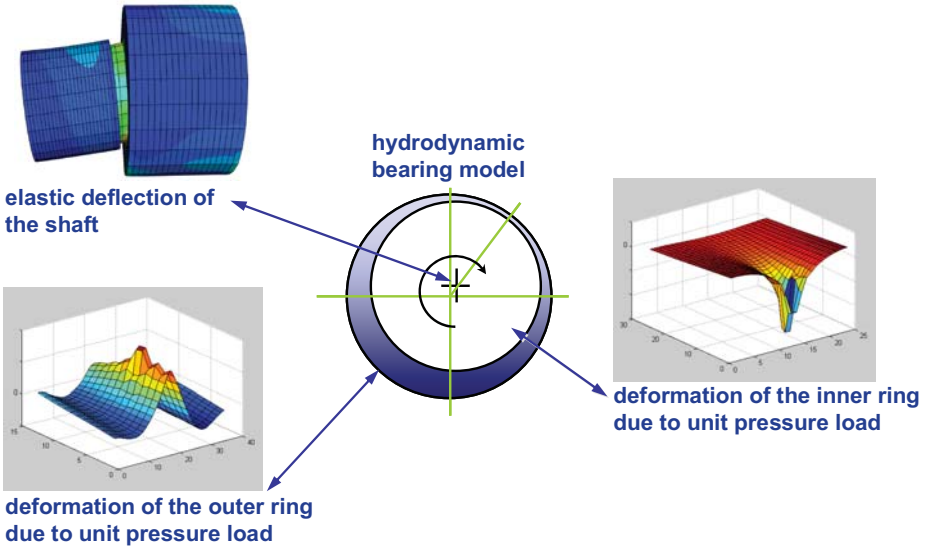

Figure 2. Structure of EHD-bearing with included deformation of the mechanical components.

With separate Finite Element models for the inner ring plus trunnion and the outer ring with the housing the deformation of the contact surfaces as reaction on the lubricant pressure will be calculated. The pressure distribution of the lubricant depends on the operating point and certainly on the size and geometry of the lubricant film what again depends on the surface deformation and has an influence on the load capacity.
As the pressure distribution can not be calculated explicitly for a general bearing geometry, iterative numerical methods have been used. In each iteration step, the complete deformation must be determined what causes very long computing times if the Finite Element model must be solved each time.
To avoid this, the method of influence functions has been used where the deformations have to be calculated only once. Herewith, a quick and efficient determination of the exact deformation of the bearing due to the pressure distribution can be done. This drastically reduces the overall computing times. Figure 3 shows such an uncouple program sequence.

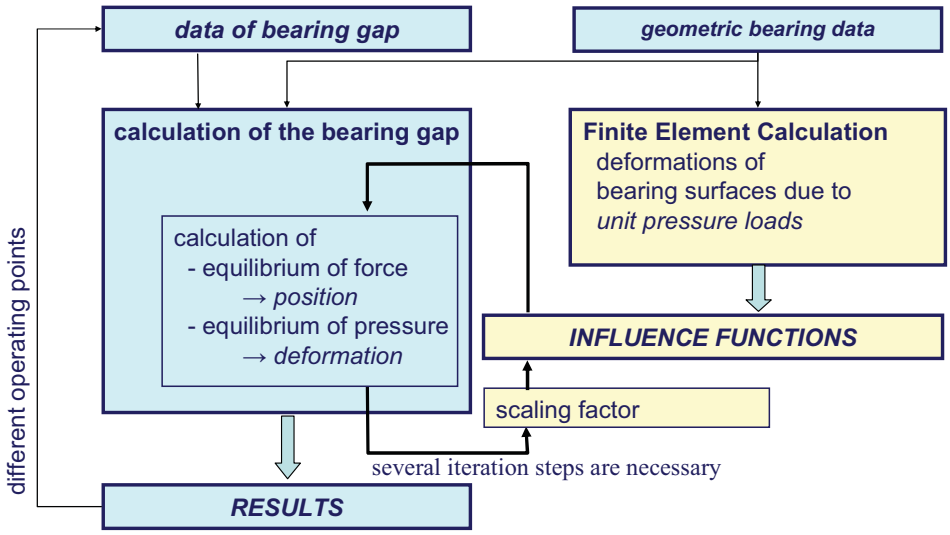

Figure 3. Uncoupled program sequence for calculation of the bearing gap.

3 Finite Element model for the calculation of the elastic deformations

A necessary requirement for the permissibility of influence functions describing the elastic deformations is the linear relationship between the pressure in the lubricant film and the resulting deformations of the mechanical components.

The next step for this approach is the splitting of the contact surface into a grid. The influence functions will be generated by applying unit pressure loads on an element of the bearings surface and analysing the resulting deformations – see Figure 4. In our case Finite Element models have been used for these calculations, where the unit pressure loads were applied separately on each surface element of the model mesh. Because of the above mentioned linear relationship, the total deformation - as the result of the total pressure distribution – easily can be calculated by scaling and summing up of the results of the single unit pressure loads.

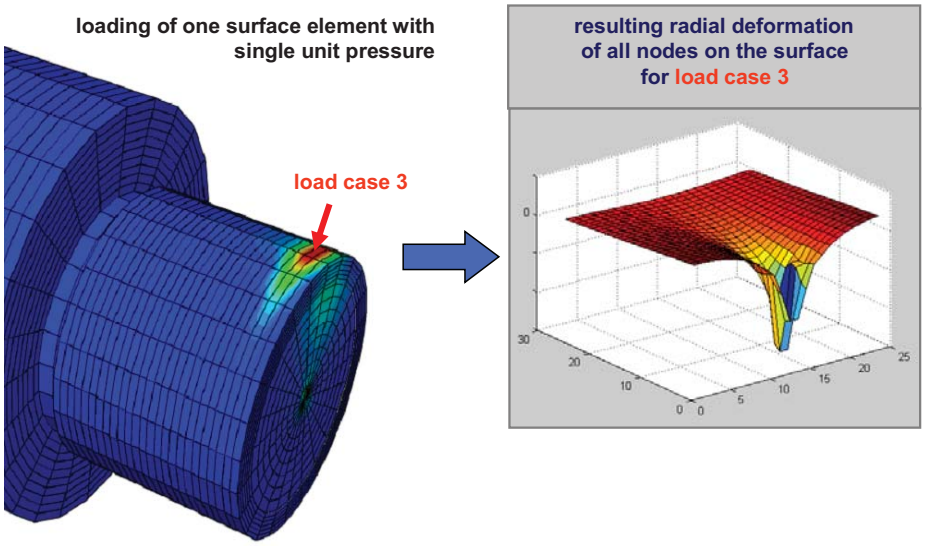

Figure 4. Single unit pressure on a surface element of the inner ring and the resulting radial deformations

The trunnion and the outer ring of the hydro-dynamic bearing are only coupled via the fluid in the bearings gap, what allows the use of independent mechanical models for both components. A special aim of the corresponding research project also was to automate the calculation of the influence matrices (influence functions evaluated at the surface elements of the model mesh) by an automatic generation of the input files for the Finite Element calculations and an automatic evaluation of the final results.

For our application the trunnion is a rotationally symmetrical part. Hence it can be described by a very simple geometry what enables a fully automatically generation of the Finite Element model including the nodes of the mesh. This again simplifies the evaluation of the results, because the node definitions, which are needed for the determination of the surface deformations, are known a priori. A second advantage of this rotationally symmetrical model was that the specific load cases only have to be applied on one row of elements with the same angular position on the cylindrical surface.

The outer ring of the bearing including the housing has been modeled to allow an implementation of realistic boundary conditions which have significant influence on the deformation of the inner surface of the ring. For this complex 3D model an automatic generation of the nodes of the mesh was no longer possible because the simplifications and advantages of the trunnion model were no longer valid. Thus, the existing 3D Finite Element models for the outer ring and the housing have been used for the generation of the input files including all the boundary conditions and forces.

4 Pressure distribution of the transient deformed bearing

4.1 Conditions for modelling

Analysing the bearing gap it is supposed that the bearing is void of any hydrostatic influence. For the determination of the dynamic influences at the operating point correct assumptions have to be made for exactly this point. Not only the ideal position of the trunnion had to be modelled, but also an instable one. The model also calculates and considers the adjustment of the inner ring in relation to the outer ring in axial direction and only on the vertical plane.

In order to investigate the reaction of the bearing an instationary view is necessary. Furthermore, the existence of a finite bearing is assumed. As a result the simplified assumtions of a very narrow relation b/d < 0.25 as well as of a very wide bearing b/d > 4 does not apply [1]. Also a circle-cylindric elementary form of an inner and outer ring is assumed. The surface of such looking bearings is bare of holes and milled slots. Another point of analysis concerns the consideration of the bearings' reaction on the turning trunnion in the fixed housing.

The lubricant is assumed being an incompressible Newtonian fluid with constant viscosity. The fluid flow in the gap is assumed as laminar. This state is to be calculated by means of the Reynolds´ number. The absolute clearance ratio is defined as the difference of the diameter between the outer and the inner ring with $S = d_s - d_z$ [1]. Furthermore, the inertial force of the lubricant is neglected in favor of the viscosity as well as the gravitation force and buoyancy. Due to the insignificant height of the bearing gap in relation to the other overall geometry the pressure in the direction of the bearing gap is assumed being constant. The model should enable the analysis of translatory but not rotatory vibrations of the trunnion. Therefore, the second derivation of the lubricants velocity in the direction of the bearing gap is significantly higher than in axial direction. An important assumption concerns the adhesion on the ideale plane surface.

4.2 Geometry of bearing gap

Following – already above mentioned – parameters are taken into account in order to calculate the resulting geometry of the bearing gap:

- Dislocation of rigid bodies of the inner and outer ring
- Inclination of the trunnion on the vertical plane
- Deflection of the trunnion
- Deformation in radial direction of the inner and outer ring´s surfaces which have contact with lubricants

The dislocation of the rigid bodies in particular of the inner and outer rings have been defined by the excentricity of the bearing. This excentricity is much smaller than the radii of the both rings (E<<R and E<<r). Under this prerequisite the radial height of the bearing gap can be simplified as following:

$$h(\varphi_{local}) \cong R - r + e\cos(\varphi_{local}) \tag{1}$$

For the local angle of the bearing gap does apply:

$$\varphi_{local} = \varphi_{global} - (\varphi_{\min} + \pi) \tag{2}$$

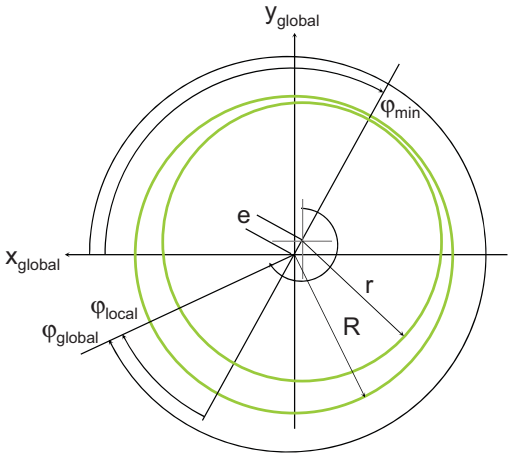

Figure 5. Geometry and angle of bearing gap.

The bearings gap will also change due to the vertical adjustment which contains the deflection and a superposed inclination of the trunnion. For this the deflection will be calculated with the FE model and will be used later with the influence functions. To identify the resulting displacement of the axis the calculated deflection $\delta_{deflection}$ will consequently superpose with the inclination φ_{slant} as well as a correction factor $\varphi_{correction}$.

$$\delta(z) = z\sin(\varphi_{slant} + \varphi_{correction}) - \delta_{deflection} \tag{3}$$

Thereby the correction angle includes possible inclination of the housing. To obtain the absolute adjustment of all points of the center line the effect of displacement of the axis $\delta_{(Z)}$ consolidates with the radial displacement of trunnion with the value e in direction of φ_{min} must be taken into account.

$$e_{slant}(z) = \sqrt{e^2 + \delta(z)^2 - 2e\delta(z)\cos\left(\frac{5}{2}\pi - \varphi_{\min}\right)} \tag{4}$$

This adjustment and the change of the angle for the minimum bearing gap reads as

$$\eta = \arccos\left(\frac{-\delta(z)^2 + e^2 + e_{slant}{}^2}{2e_{slant}e}\right) \tag{5}$$

and is shown in Figure 6. Regarding these effects the height of the bearing gap of equation (1) must expand.

$$h = R - r + e_{slant}\cos(\varphi_{global} - \varphi_{\min} + \eta + \pi) \tag{6}$$

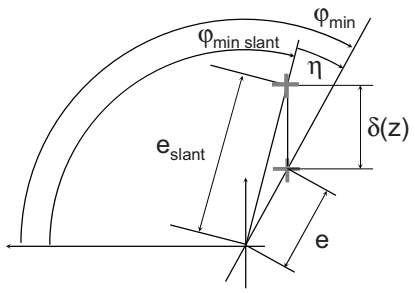

Figure 6. Adjustment of axis according by deflection and inclination of the trunnion.

4.3 Using Reynold's differential equation for model of bearing gap

To calculate the bearings gap the Reynold differential equation will be used. By applying the Finite-Difference Method these differential equations can be resolved. Fundamental equations of the calculation for the distribution of pressure in the bearing gap are the dimensionless Reynold differential equation for the unsteady state.

$$\frac{\partial}{\partial\varphi}\left(H_V{}^3\frac{\partial p}{\partial\varphi}\right) + \left(\frac{D}{B}\right)^2\frac{\partial}{\partial Z}\left(H_V{}^3\frac{\partial p}{\partial Z}\right) = \frac{6\eta}{\Psi^2}\left(\omega_B\frac{\partial H_V}{\partial\varphi} + 2\frac{\partial H_V}{\partial t}\right) \tag{7}$$

Following dimensionless parameters are used in equation (7):

$$H_v = \frac{h_V}{\Delta R} \qquad \Sigma = \frac{\Delta R}{R} \qquad Z = \frac{z}{\frac{B}{2}} \tag{8}$$

For this dimensionless parameters the radius R and width B of the bearing are required as well as the height of bearing gap h_v. This height contains the geometry of the bearing gap, described in the previous chapter and the radial elastic deformation of mechanical components of the bearing v_r, also calculated with the finite element model and again included later with the influence functions in the ongoing calculation.

$$h_V(\varphi_{local}, z) = h(\varphi_{local}, z) + v_r(\varphi_{local}, z) \tag{9}$$

Next step is the implementation of the dimensionless coefficient of pressure Π. With this coefficient a transformation with Sommerfeld will be executed $\overline{\Pi}$.

$$\Pi = p\frac{\Psi^2}{\omega_B\eta} \tag{10}$$

$$\overline{\Pi} = \Pi H_V{}^{\frac{3}{2}} \tag{11}$$

With these parameters the differential equation for pressure can be set up.

$$\frac{\partial^2 \overline{\Pi}}{\partial \varphi_{local}{}^2} + \left(\frac{D}{B}\right)^2 \frac{\partial^2 \overline{\Pi}}{\partial Z^2} + a\overline{\Pi} = b$$

$$a = \frac{15}{4} H_V^{-\frac{5}{2}} \left(\frac{\partial H_V}{\partial Z}\right)^2 - \frac{3}{4} H_V^{-\frac{5}{2}} \left(\frac{\partial H_V}{\partial \varphi_{local}}\right)^2 - \frac{3}{2H_V}\left(\frac{\partial^2 H_V}{\partial \varphi_{local}{}^2} + \frac{\partial H_V}{\partial Z} + \frac{\partial^2 H_V}{\partial Z^2}\right) \tag{12}$$

$$b = 6 H_V^{-\frac{3}{2}} \frac{\partial H_V}{\partial \varphi_{local}} + \frac{12}{\omega_B} H_V^{-\frac{3}{2}} \frac{\partial H_V}{\partial t}$$

For the boundary conditions of these differential equations applies the zero value of the borders. This means the border of the beginning $\varphi = \varphi_1$ and end $\varphi = \varphi_0$ of the distribution of pressure, as well as both ends of the bearing $Z = 0$ and $Z = B$.

$$\Pi(\varphi_1, Z) = 0 \quad \Pi(\varphi_0, Z) = 0 \quad \Pi(\varphi, Z = 0) = 0 \quad \Pi(\varphi, Z = B) = 0 \qquad \left.\frac{\partial \Pi}{\partial \varphi_{local}}\right|_{\varphi=\varphi_0} = 0 \tag{13}$$

To dissolve the differential equations for pressure the bearing gap has been discretised in angular and in axial direction to form a rectangular grid with factors of grid ΔZ and Δφ. The pressure on every point of grid is ascertained approximately numerically replacing the derivation via differential quotient.

$$\left.\frac{\partial \overline{\Pi}}{\partial Z}\right|_{i,j} = \frac{\overline{\Pi}_{i+1,j} - \overline{\Pi}_{i-1,j}}{2\Delta Z} \qquad \left.\frac{\partial \overline{\Pi}}{\partial \varphi_{local}}\right|_{i,j} = \frac{\overline{\Pi}_{i,j+1} - \overline{\Pi}_{i,j-1}}{2\Delta \varphi_{local}}$$

$$\left.\frac{\partial^2 \overline{\Pi}}{\partial Z^2}\right|_{i,j} = \frac{\overline{\Pi}_{i+1,j} - 2\overline{\Pi}_{i,j} + \overline{\Pi}_{i-1,j}}{\Delta Z^2} \qquad \left.\frac{\partial^2 \overline{\Pi}}{\partial \varphi_{local}{}^2}\right|_{i,j} = \frac{\overline{\Pi}_{i,j+1} - 2\overline{\Pi}_{i,j} + \overline{\Pi}_{i,j-1}}{\Delta \varphi_{local}{}^2} \tag{14}$$

Hence, it is possible to form the equation for the pressure on every point of grid with reference to the pressure of the neighboring points of the grid.

$$\overline{\Pi}_{i,j} = \frac{b\left(\Delta\varphi^2 \Delta Z^2 B^2\right) - \left(\overline{\Pi}_{i,j+1} + \overline{\Pi}_{i,j-1}\right)\left(\Delta Z^2 B^2\right) - \left(\overline{\Pi}_{i+1,j} + \overline{\Pi}_{i-1,j}\right)\left(\Delta\varphi^2 D^2\right)}{a\left(\Delta\varphi^2 \Delta Z^2 B^2\right) - 2\Delta Z^2 B^2 - 2\Delta\varphi^2 D^2} \tag{15}$$

If some point outside the area of pressure is needed, this value is set as zero.

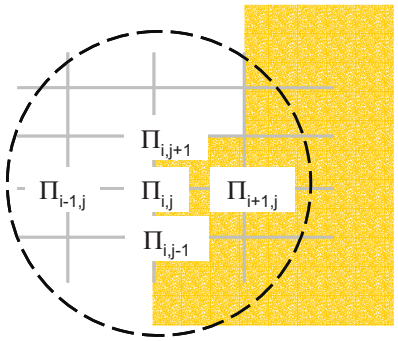

Figure 6. Differential equation of each point of grid at pressure area.
(pressure area illustrate in yellow colour)

All equations for the points of the grid inside the area of pressure can be summarised into the following matrix form.

$$\underline{A} \cdot \vec{\overline{\Pi}} = \vec{\beta} \tag{16}$$

The equation above with only few items in the matrix A can be solved numerically by the conjugate gradients squared method. Herewith, the pressure distibution of the deformed bearing easily can be calculated.

4.4 Definition of pressure area for deformed bearing

The definition of the pressure area so far and the corresponding boundary conditions apply for an undeformed bearing which is not slanted. In this case the pressure distribution starts at the angle with the minimum height of bearing gap and ends in the area just over the maximum height of the gap. Considered over the width these both straight lines of the minimum and maximum heights of bearing gaps will turn to curves, if the bearing is deformed and slanted. These limiting curves φ_{hmax} and φ_{hmin} are determined by the calculation of minimum and maximum height of bearing gap on the basis of the grid line in circumferential direction. The above mentioned equation system is set up for all points of the grid, which are situated within these boundary curves.

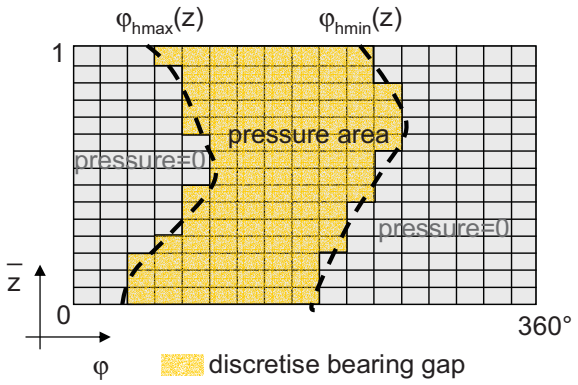

Figure 7. Discretise pressure area of deformed and slant bearing

4.5 Identification the position of shaft at a defined operating point

The assumed forces of the model correspond to the forces which work on the bearing in reality and apply at a certain desired operating point. By variation of the eccentricity and its direction the distribution of pressure can be adjusted to such an extent that the generated reaction force of the bearing is poised in equilibration with the outer forces which work on the bearing. The searched position of the trunnion is calculated iteratively.

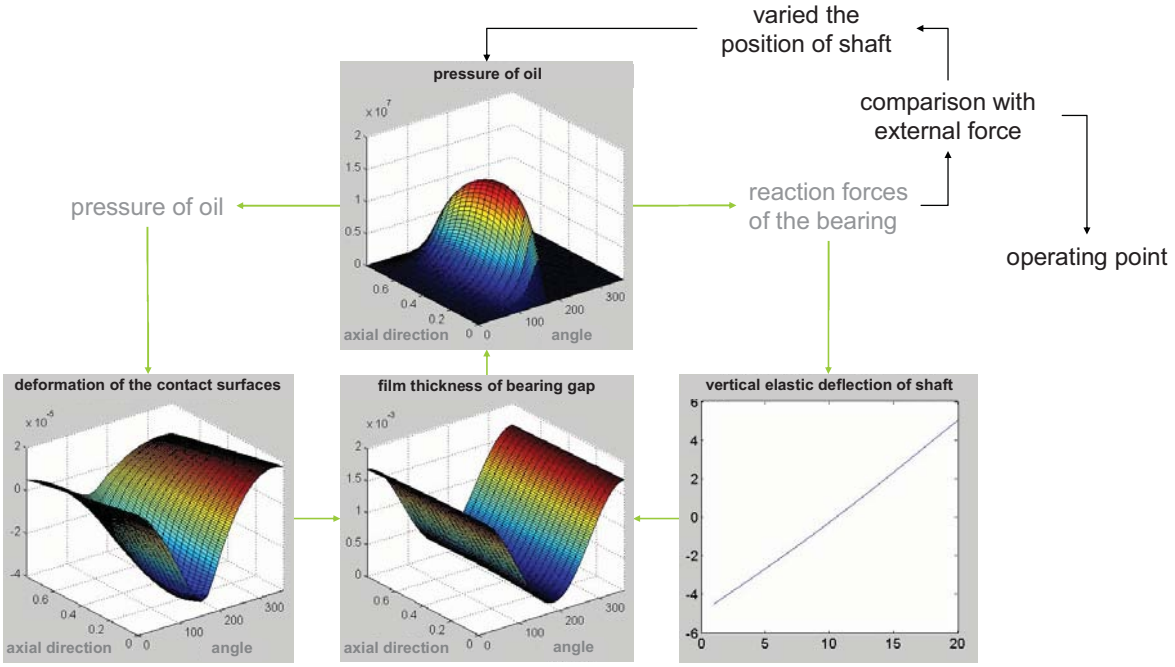

Figure 8. Procedur to identify the position of shaft at a defined operating point

Based on the position of the trunnion determined in the operating point, the stiffness and damping matrixes are approximately calculated by means of differential quotients. The horizontal and vertical position of the trunnion and its velocity as well as the slanting position are variied, and the changed vertical and horizontal components of the reaction force of the bearing and the changed moment of the bearing can be determined.

5 Summary

With this paper, the backgrounds of an Elasto-Hydrodynamic (EHD) bearing and a way to set up an appropriate simulation model as well as its implementation have been presented. It described a procedure for an independent calculation of the deformation of the mechanical components and the pressure of the lubricant inside the bearing gap by using influence functions and the principle of superposition. The used geometry of the bearing gap is shown by including the deformation and slunt of the bearing. Looking forward, the presented procedure for the calculation of the hydrodynamic bearing should be extended by hydrostatic effects.

6 References

[1] Lang O.R., Steinhilper W.: Gleitlager; Springer 1978.

[2] B. Winkler, G. Mikota, R. Scheidl, B. Manhartsgruber: Modeling and Simulation of the Elasto-Hydrodynamic Bahavior of Sealing Gaps, Australien Journal of Mechanical Engineering, Vol. 2, No. 1.

[3] J.S. Rao, M. Saravanakumar: Numerical Simulation of Seal FLow and Determination of Stiffness and Damping Coefficients, 7th IFToMM-Conference on Rotor Dynamics, Vienna, Austria, 25-28 September 2006.

[4] Th. Christ, H. Irretier, Th. Kreuzinger-Janik: Entwicklung eines Berechnungsprogrammes zur Ermittlung der Steifigkeits- und Dämpfungskoeffizienten von Gleitlagern, Diplomarbeit am Institut für Mechanik, U-niversität Gesamthochschule Kassel, 1999.